第18回性能に基づく橋梁等の耐震設計に関する
シンポジウム講演論文集（2015年7月）

Evaluation on the Pullout of Longitudinal Bar by Comparison between Different Reinforced Full-scale RC Columns Based on E-Defense Excitation

Heng GAO[1] ・ Kenji KOSA[2] ・ Tatsuo SASAKI[3]

[1]Student Member of JSCE, Graduate Student, Graduate School of Engineering, Kyusyu Institute of Technology
(〒804-8550 Sensui-cho 1-1, Tobata-ku, Kitakyushu, Fukuoka)
[2]Member of JSCE, Ph.D., Professor, Department of Civil Engineering, Kyusyu Institute of Technology
(〒804-8550 Sensui-cho 1-1, Tobata-ku, Kitakyushu, Fukuoka)
[3]Member of JSCE, M.Eng., Manager, Technical Generalization Division, Nippon Engineering Consultants Co., Ltd.
(Currently in the doctoral program at Kyushu Institute of Technology)

1. INTRODUCTION

A 3D shake table experiment on a large-scale reinforced concrete bridge using E-Defense has been constructed by the National Research Institute for Earth Science and Disaster Prevention. With the facilities for E-Defense, a series of anti-seismic experiments of bridges has been conducted, among which full-scale RC columns named C1-1[1)] and C1-5[2)] have been constructed shown in Fig. 1. Columns as the type of C1-1 built in the 1970s has been widely damaged during 1995 Kobe Earthquake. However, column C1-5 designed with 2002 JRA specification behaved satisfactorily under a near-field ground motion recorded during the 1995 Kobe Earthquake.

The objective specimens were designed for evaluating flexural failure. Response displacement of an RC column, which contributes to the development of lateral displacement of the deck, is not only caused by flexure but also rotation induced by the longitudinal bar pulling out from the inside footing. It is defined hereinafter as pullout. Our former research[3)] has paid attention to the C1-1 specimens, and it is clarified that the pullout has contributed great (about 30%) to the column top displacement and tri-layer of C1-1 has contributed to the pullout with the bar-to-bar reduction influence. This paper will pay attention to the comparison between different reinforced C1-1 (tri-layer) and C1-5 (bi-layer) to evaluate their different behavior in pullout.

In the shake table experiment of C1-1 and C1-5, the displacement meter (LVDT) at the base and the strain gauge (SG) attached on the longitudinal bars are referred to for measuring the pullout displacement.

The experimental data of pullout displacement by LVDT and SG is summarized firstly in Chapter 3. Moreover, to reveal the different behavior of C1-1 and C1-5t in pullout and it contributed ratio for column displacement, the part of pullout-induced column displacement is solved. In order to clarify the mechanism of pullout and bar-to-bar reduction in different reinforced C1-1 and C1-5, analysis is conducted based on the theoretical equation provided former research[4)] in Chapter 4. Bar-to-bar reduction coefficient is also defined in this Chapter. Study flow can be shown as Fig. 2 shows.

Fig. 1 Shake Table Test Using E-Defense

2. EXPERIMENTAL SETUP

(1) C1-1 Specimen

In this Section, the setup of C1-1 will be explained.

As Fig. 3 shows, the column was constructed by tri-layer of reinforcement of 29mm diameter, 32, 32 and 16 bars at outer, middle and inner layers respectively. Deformed circular stirrups of 13mm diameter are provided at 300mm intervals. At the top zone of 1.15m and at the base zone of 0.95m length, outer ties are provided at 150mm intervals. Stirrups are lap spliced at 390mm. The longitudinal reinforced ratio was 2.02%, and the tie volumetric reinforced ratio for the middle was 0.32% and for the top or base was 0.42%. On the day of the experiment, the yield strength of the longitudinal bars, stirrups and concrete were measured as 366 MPa, 193 MPa and 33 MPa.

Strain gauges were attached to the longitudinal bar shown in Fig. 3 and provided at 300 mm intervals. In both the transverse and bridge axis direction, the SG was attached to the outer, middle and inner bar as shown in Fig. 1(b). As for the displacement meter at base, the series of LVDT was set at the base by both sides of the transverse and bridge axis direction. The first meter was set at 80mm height and the others are provided at 200 mm intervals.

(2) C1-5 Specimen

Different from C1-1, the column was constructed by bi-layer of reinforcement of 35mm diameter, 36 and 36 bars at outer and inner layers respectively. Deformed circular stirrups of 13mm diameter are provided at 150mm intervals. Stirrups are lap spliced at 390mm. The longitudinal reinforced ratio was 2.19%. On the day of the experiment, the yield strength of the longitudinal bars and concrete were measured as 364 MPa and 36 MPa.

Similar to the C1-5, strain gauges were attached to the longitudinal bar shown in Fig. 4 and provided at 300 mm intervals below -150mm from base. In both the transverse and bridge axis direction, the SG was attached to only outer bar as shown in Fig. 4(b). Displacement meter is set as same as C1-1

3. GENERAL EXPERIMENT DATA of C1-1

This chapter summarizes the general experimental data. The column top displacement was measured by three-dimensional displacement meter attached to the column top. To reveal the actual effect of the pullout on column top displacement, the pullout-induced part was solved.

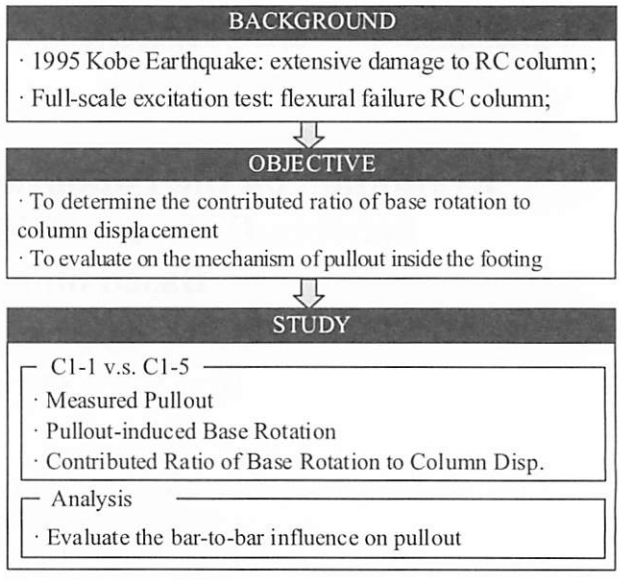

Fig. 2 Study Flow

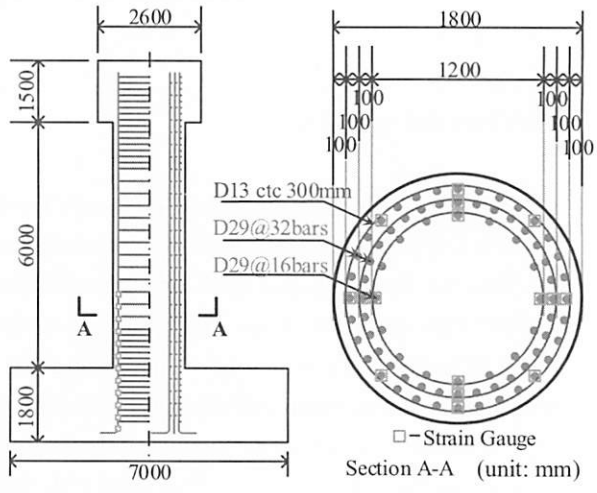

Fig. 3 C1-1 Column on E-Defense

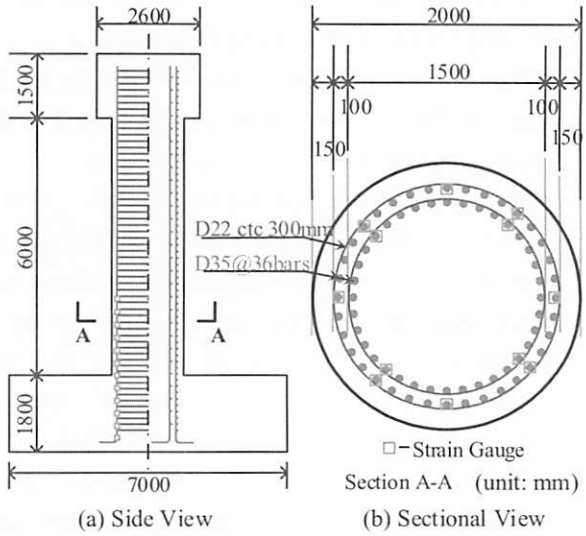

Fig. 4 C1-5 Column on E-Defense

Experimental data based on the column top was plotted initially by the load-displacement (P-δ) relationship in Fig. 5. As for C1-1 specimen, the maximum load was about 1390 kN and 1660 kN respectively in the bridge axis (East-West) and the transverse (North-South) direction. In transverse and bridge axis directions, column displacement have exceeded 0.1m and 0.15m respectively.

(1) Determination of Measured Pullout Displacement

Column displacement caused by pullout will be distinguished based on Fig. 6 which explains the procedure to solve the pullout-induced column displacement.

When the displacement of column top reaches yield displacement (1δy) towards south marked as S1, the corresponding pullout displacement at south side is marked as u_{n1} (n: north; 1: 1δy). The definition of yield displacement of column top is explained by Fig. 7. Illustrated by Fig. 7 (a), at 9.795s the strain of longitudinal bar at north side becomes yield (1896μ) and the column displacement towards south side at this time is defined as yield displacement (δy) reaching 0.049cm. The measured displacement by both LVDT and SG, shown in Fig. 7 (b), can be got by the same time at 9.795s. Similarly, the state of 2δy is marked at 12.515s when column displacement reaches twice of yield displacement.

As it is stated above, the measured pullout is solved as u_{n1} in Fig. 6 firstly. Secondly, the neutral axis, marked as X_0 in Fig. 6 (b), is solved by the cross-section calculation. Thirdly, with the measured pullout (u_{n1}) and neutral axis (X_0), base rotation can be solved ($\tan\theta = u_{n1} / X_0$). Finally, the part of column displacement caused by pullout can be solved by the base rotation and height of column ($\delta_{S1\text{-pullout}}$

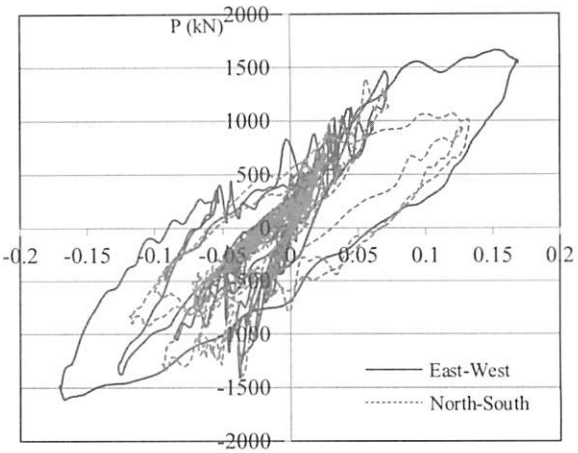

Fig. 5 Load-Displacement relationship of top of C1-1

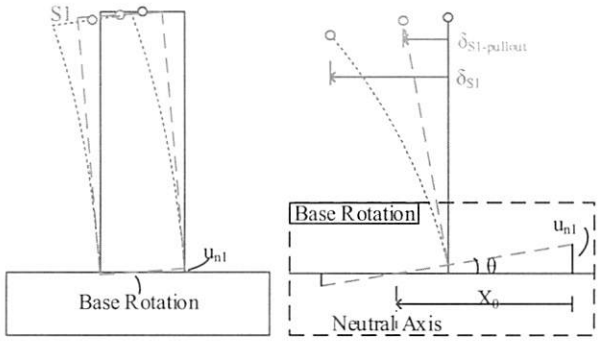

(a) Measured data about pullout

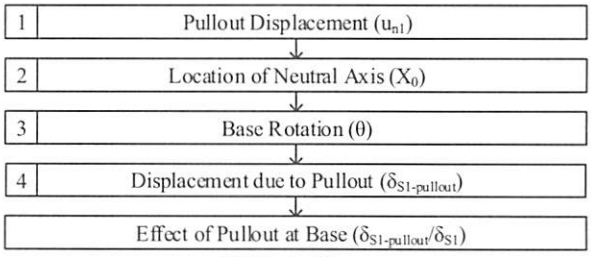

(b) Study flow

Fig. 6 Measured data and study flow

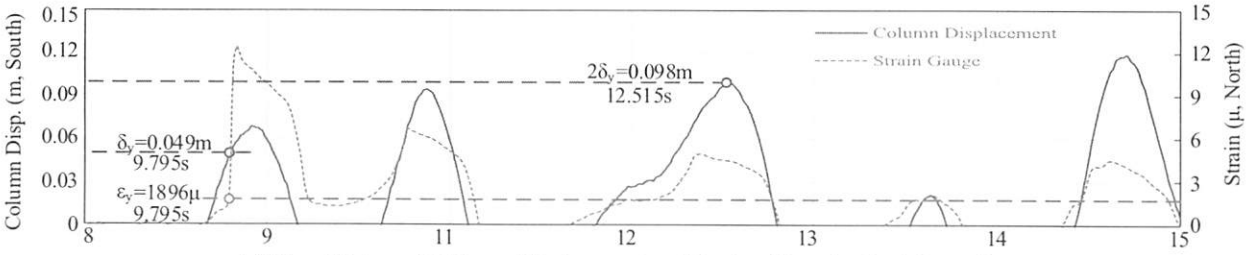

(a) Time History of Column Displacement and Strain of Longitudinal Bar at Base

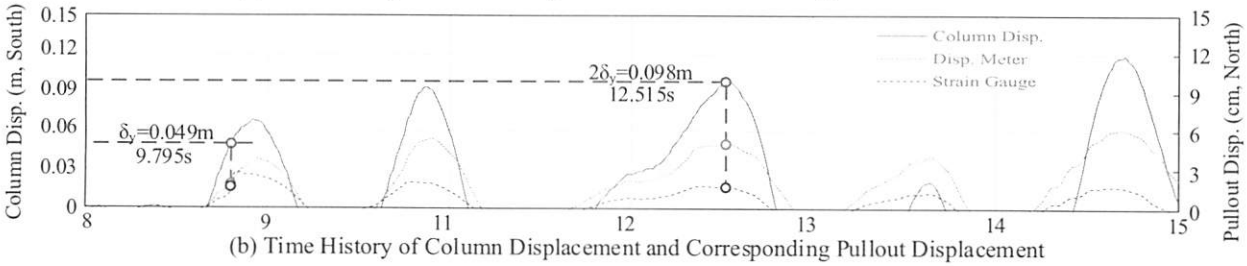

(b) Time History of Column Displacement and Corresponding Pullout Displacement

Fig. 7 Measured Pullout Displacement

$= u_{n1} / X_0 \times 7.5$ m). The contributed ratio by pullout displacement in column displacement ($\delta_{S1\text{-pullout}}$) takes in the total one (δ_{S1}) is solved to reveal the actual effect of pullout at base.

(2) Measured Pullout and Contributed Ratio

Based on the definition of yield displacement shown in Fig. 7, Fig. 8 makes a general summary of measured pullout by both LVDT and SG. The pullout displacement increases gradually along the top displacement increases. Measured pullout at 1δy reached about 1 mm and the data at 2δy varies from 1.09 mm ~ 4.95 mm. Fig. 9 is plotted to evaluate on the varied measured pullout.

Illustrated by Fig.9, taking the north as an example, when the column displacement reaches yield (1δy, marked as N1) the column top is located on the NS axle so that the measured pullout at south has been determined by column displacement towards south only. However, as for the column displacement towards west at 1δy and 2δy (marked as W1 and W2), the location of column top is close to NS axle but EW axle so that the measured pullout at east side has been determined by column displacement towards south. Moreover, the W1 and W2 seem close to each other so that the measured pullout at east side has not increased obviously leading to the measured data lower than others.

Based on the measured pullout shown in Fig. 8, the ratio of pullout-induced column displacement can be plotted in Fig. 10 with the study flow in Fig. 6. As shown in Fig. 10, pullout at base has contributed 28% to the top displacement in average during 1δy ~ 2δy. As the pullout displacement measured by strain gauge has been solved based on the integral of measured strain distribution, it shows the contributed ratio by pullout in column displacement reaches 19% which is a little smaller than that of displacement meter.

To sum it up, pullout displacement measured by displacement meter reaches 1.35 mm and 3.79 mm in average at 1δy and 2δy respectively. Meanwhile, the pullout displacement by the integral value with strain gauge reaches 1.04 mm and 3.25 mm in average at 1δy and 2δy respectively. It can be obtained that the measured pullout increases by about 3 times when the column top displacement increases by twice. However, the contributed ratio by pullout keeps steady and reaches 28% in average. On one hand, it may be caused by increased distance of neutral. On the other hand, cracks on the pier body becomes more and larger after the column displacement exceeds yield displacement.

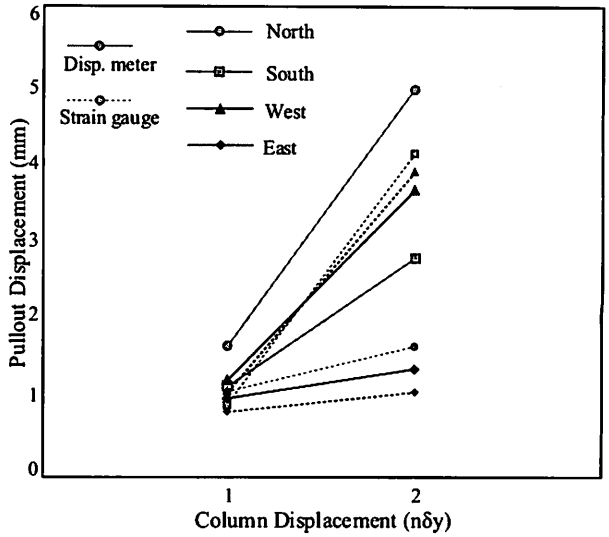

Fig.8 Measured Pullout in C1-1

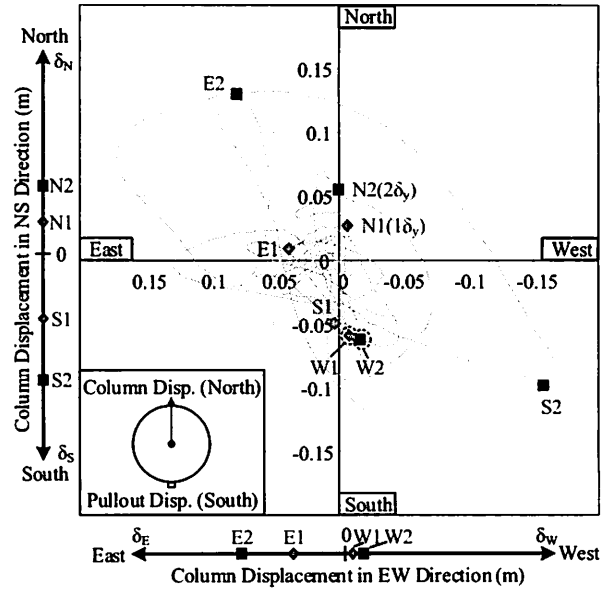

Fig.9 Orbit of Column Top (C1-1)

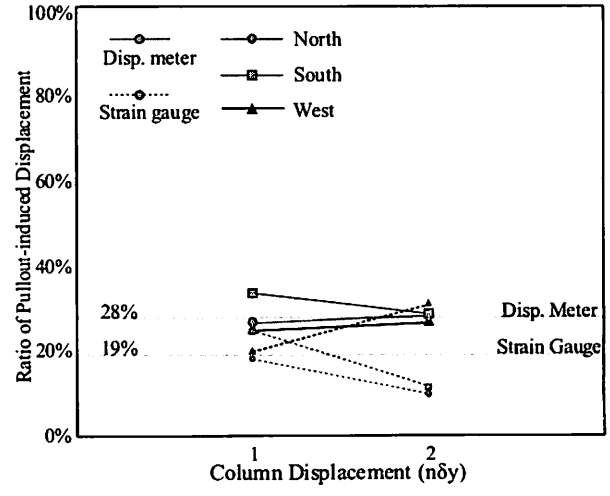

Fig.10 Contributed Ratio of Base Rotation in C1-1

4. GENERAL EXPERIMENT DATA of C1-5

(1) Measured Pullout and Its Contributed Ratio

Experimental data based on the C1-5 specimen was plotted initially by the load-displacement (P-δ) relationship in Fig. 11. The maximum load in experiment of C1-5 has reached 1682 kN and 2445 kN respectively in the bridge axis (EW) and the transverse (NS). Column displacement, in transverse and bridge axis directions, has exceeded 0.107 m and 0.124 m respectively.

Similar to the C1-1, based on the definition of yield displacement shown in Fig. 7, Fig. 12 makes a general summary of measured pullout by both LVDT and SG. The pullout displacement increases gradually along the top displacement increases. Measured pullout at 1δy reached about 1.5 mm and the data at 2δy reached about 4.5 mm.

Different from C1-1, the measured pullout displacement roughly accords with each other in C1-5 by the almost same increasing trend. Illustrated by Fig. 13, the column top at 1δy has located closely to the axle so that the measured pullout has not been affected by the column displacement towards other direction. Moreover, the location of column top at 1δy and 2δy do not close to each other as the W1 and W2 in C1-1 so that the pullout of displacement at corresponding side keeps increasing.

Based on the measured pullout plotted in Fig. 12, the actual effect of pullout at base in C1-5 with reinforcement of bi-layer can be explained by Fig. 14. As shown in Fig. 12, pullout at base has contributed 30% to the top displacement on average during 1δy ~ 2δy. However, pullout displacement measured by strain gauge shows the contributed ratio by pullout being 23% which is a little smaller than that of displacement meter.

(2) Evaluation of Experimental Data by C1-5

To sum it up, pullout displacement measured by displacement meter reaches 1.59 mm and 4.85 mm in average, and by strain gauge reaches 1.24 mm and 3.12 mm in average at 1δy and 2δy respectively. It can be also obtained that the measured pullout increases by about 3 times when the column top displacement increases by twice. However, the contributed ratio by pullout keeps steady and reaches 30% in average. Although C1-1 and C1-5 has been reinforced differently based on different code, them seems to have similar behavior on the pullout and it-induced column top displacement.

Pullout in C1-5 seems greater than C1-1. However, as the C1-5 (diameter of 2 m) has a larger scale than C1-1

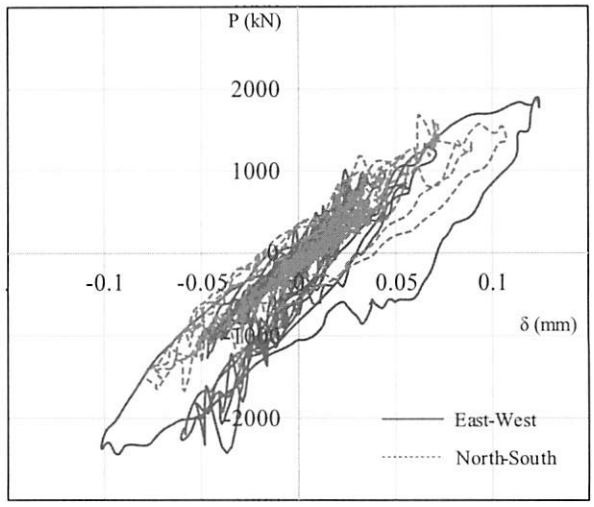

Fig.11 Load-Displacement relationship of top of C1-5

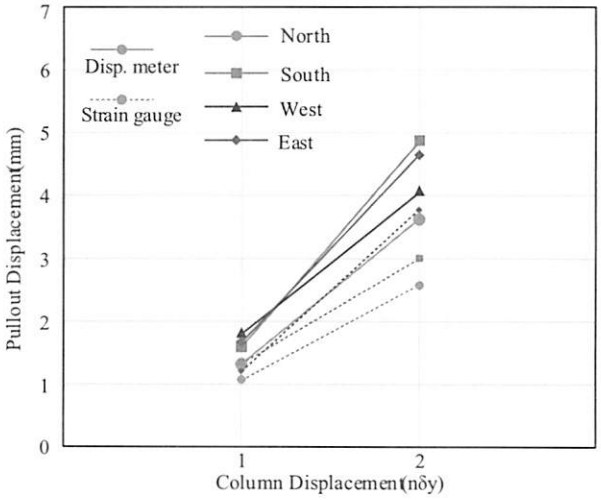

Fig.12 Measured Pullout in C1-5

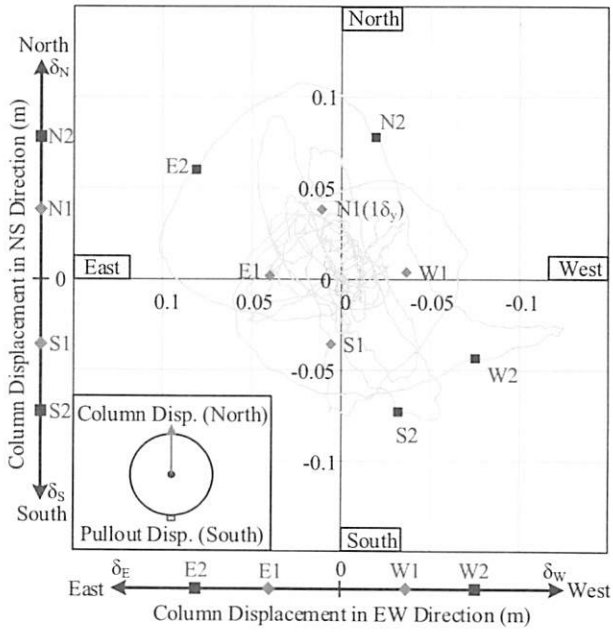

Fig.13 Measured Pullout in C1-5

(diameter of 1.8 m), the natural axle of C1-5 (1δy: 1.16 m; 2δy: 1.36 m) is also bigger than that of C1-1 (1δy: 0.97 m; 2δy: 1.3 m). Consequently, the base rotation and it-induced column displacement in both C1-1 and C1-5 is also same with each other. Moreover, according to the yield displacement shown in Fig. 9 and Fig. 13, both of C1-1 and C1-5 have reached 0.038m averagely. With the almost same pullout-induced column displacement, the contributed ratio by pullout takes about 30% steadily.

Consequently, the pullout cannot be neglected with the relative great contributed ratio reaching 30% and various influence factors have effect on the pullout so that its mechanism should also be discussed further to evaluate on the influence factor on pullout.

5. EVALUATION OF THE INFLUENCED FACTOR ON PULLOUT

(1) Analysis Based on Strain Distribution

Based on the measured data displacement meter and strain gauge in Chapter 4, pullout contributed to the response column displacement by about 30%. In this chapter, the mechanism of pullout is evaluated based on experimental data and analysis.

Strain distribution of C1-1 at 1δy along the longitudinal bar inside the footing (from -1.5 m to 0 m) has been plotted in the Fig. 15 (a). Similarly, strain distribution (from -1.35 m to 0 m) of C1-5 has been plotted in the Fig. 16 (a). At the yield point, behavior of longitudinal bar in different side has accords with each other in both C1-1 and C1-5. However, shown in Fig. 15 (b) and Fig. 16 (b), at the time of 2δy strain distribution of direction becomes different as the longitudinal bar has exceed yield. Shown in Fig. 15 (b), the strain at base (0m) in C1-1 has reached about 17826μ and 20643μ in west and south side respectively. Moreover, as shown in Fig. 16 (b), the strain at base of C1-5 has reached 13736μ and 15540μin south and east side respectively. The analysis of next part will mainly pay attention to the south-west side in C1-1 and south-east side in C1-5 as the experimental data of outer, middle and inner layer accords with each other.

Analysis is conducted based on the calculated methods reported in the literature[3]. The following theoretical equation shows the relationship of bond stress, steel stress and slip (τ-s and σ-τ):

$$\tau / f_{ck}^{'} = 0.73(\ln(1+5000S/\phi))^3/(1+\varepsilon\times 10^5) \quad (1)$$

$$\Delta\sigma = \pi\cdot\phi\cdot\Delta x\cdot\tau / A_s \quad (2)$$

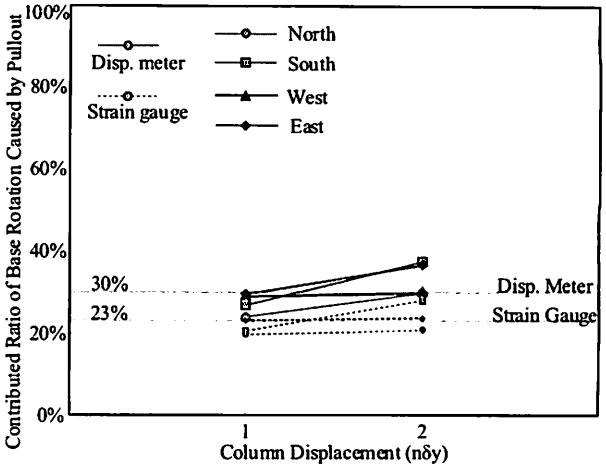

Fig.14 Contributed Ratio of Base Rotation in C1-5

Table 1 Reinforced Type of C1-1 and C1-5

	Contributed Ratio (%)	Reinforced Layer	Main Bar (Φ)	Lapped Spacing
C1-1	28	3	29 mm	156 mm
C1-5	30	2	35 mm	148 mm

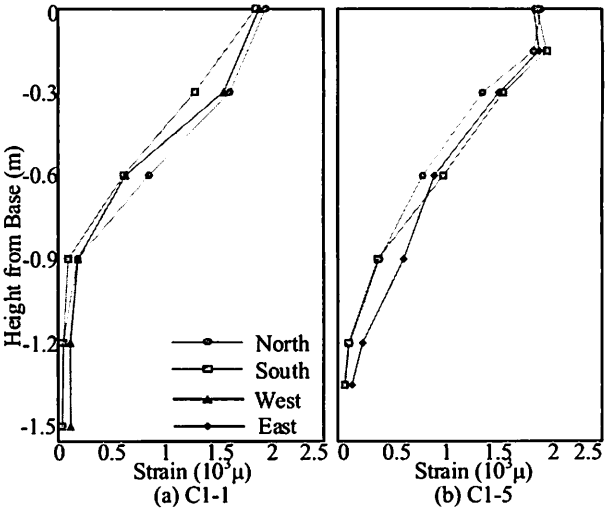

Fig.15 Strain Distribution at 1δy

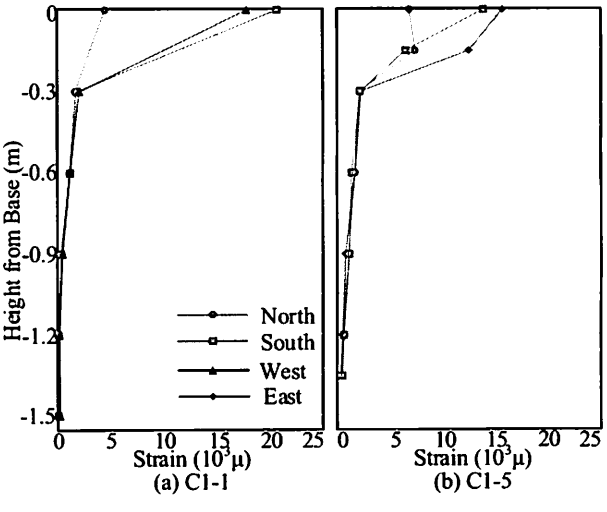

Fig.16 Strain Distribution at 2δy

Here, τ is the bond stress between concrete and steel bars; f'ck is compressive strength of concrete; S is bond slip; ϕ is the diameter of longitudinal bar; ε is strain; $\Delta\sigma$ is the increment of stress in interval of Δx.

Based on the equations listed above, analysis has been conducted and the analytical results on pullout displacement and strain distribution along the longitudinal bar inside the footing can be solved shown in Fig. 18 and Fig. 19. This kind of analysis, defined hereinafter as Case 1, has been conducted by considering a single bar, however, the C1-1 and C1-5 has been reinforced by multi-layer and the resistant area will reduce more than 30% due to the close reinforced distance. Multi-layer may contribute to the reduction influence from bar-to-bar. Another modification[4] considering this part of reduction, defined hereinafter as Case 2, has been conducted. The reduction coefficient for bond stress can be shown as follows:

$$K_i = 0.4 + 0.03 D_i / \phi \qquad (3)$$

Here, the Di is the distance between two adjacent bars and ϕ is the diameter of longitudinal bar.

The reduction coefficient for bond stress can be calculated based on the Fig. 17, in which (a) and (b) is C1-1 and C1-5 respectively. C1-1, shown in Fig. 17 (a), has been reinforced by tri-layer. One of the bars in outer layer is taken as an example, the distance between it and others bars around it varied from 100mm to 200mm. Based on Eq. (3), the component reduction coefficient can be calculated as 0.503 ~ 0.607. As for the reduction coefficient of bond stress, it is defined as product of average calculated component value by the different reinforced spacing which is calculated as 0.181 for outer layer in C1-1. Similarly, the reduction coefficient for C1-5 has also been solved, which reaches 0.201 for outer layer. Based on Eq. (1), analysis that bond stress multiplied by the reduction coefficient of 0.181 for C1-1 and 0.201 for C1-5 is conducted.

(2) Analytical Result vs. Experimental Data

The analytical results are plotted in Fig. 18 and Fig. 19 for C1-1 and C1-5 respectively based on the analytical model explained in Section 4.1. C1-1 is illustrated by Fig. 18 in which the (a) and (b) illustrate the state of 1δy and 2δy. The analytical result of strain in analysis of Case 2 has reappeared the experiment better than the analysis of Case 1. As it stated above, the C1-1 specimen is constructed by tri-layer of reinforcement. In order to evaluate the effect of multi-layer, depth of bond fracture at base is discussed based on the analytical result.

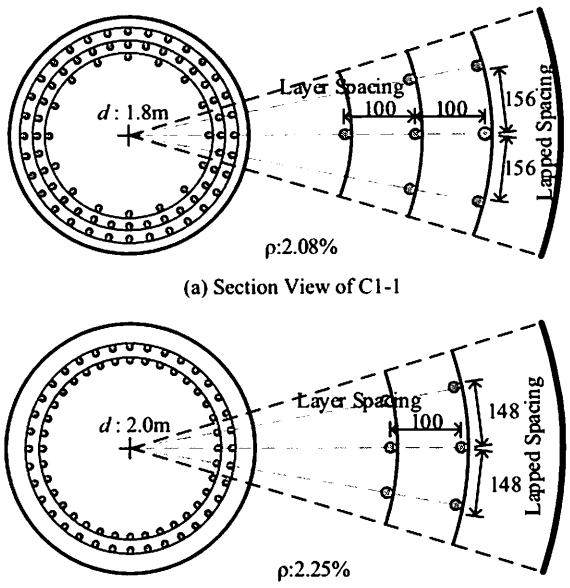

(a) Section View of C1-1

Fig.17 Strain Distribution at 1δy

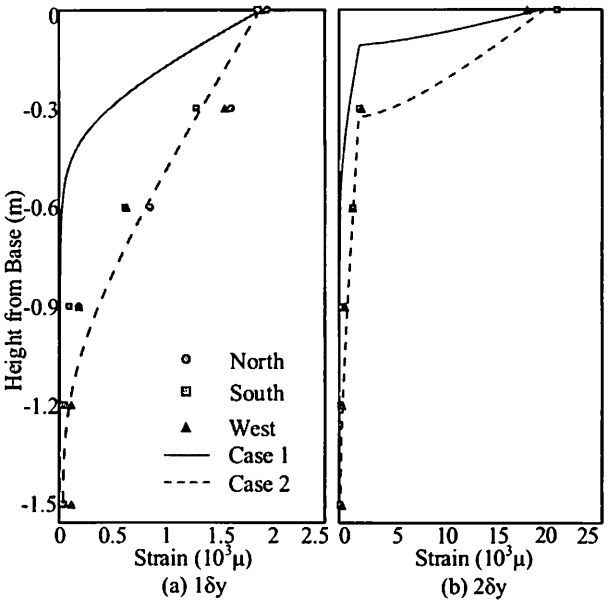

(a) 1δy (b) 2δy

Fig.18 Analytical and Experimental Data (C1-1)

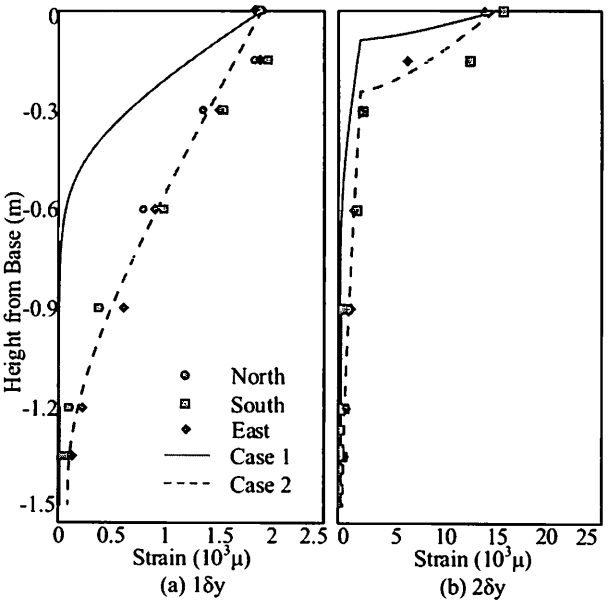

(a) 1δy (b) 2δy

Fig.19 Analytical and Experimental Data (C1-5)

According to the referenced research[3], when the bond slip (S in Eq. (1)) exceeds 0.014ϕ (= 0.014×29 = 0.406 mm), it is defined as the beginning of bond fracture depth. Based on analytical result, at 1δy, bond fracture occurs from -0.455 m and -1. 436 m to the base (0 m) respectively for Case 1 and Case 2 analysis. At 2δy, it is at -0.485 m and -1.458 m respectively for Case 1 and Case 2 analysis.

Similarly, as for the C1-5 shown in Fig. 19, the analytical result of strain in analysis of Case 2 has also reappeared the experiment better than the analysis of Case 1. Based on analytical result, at 1δy, bond fracture occurs from -0.765 m and -1.408 m to the base (0 m) respectively for Case 1 and Case 2 analysis. At 2δy, it is at -0.805 m and -1.445 m depth respectively for Case 1 and Case 2 analysis. C1-5 also shows that bi-layer of reinforcement have caused the bond fracture to begin deeper inside the footing which may lead pullout at base to become greater. Based on the comparison between C1-1 and C1-5, C1-1 seems to have deeper depth of bond fracture than C1-5 in Case 2 analysis. C1-1 which has been reinforced tri-layer which has one more layer than C1-5, in which the reduction influence from bar-to-bar become greater leading to its relative deeper depth of bond fracture.

To sum it up, analysis considering the bar-to-bar reduction has well reappeared the experimental data in both C1-1 and C1-5. Based on the comparison between analyses whether considering the bar-to-bar reduction influence, it is clarified that multi-layer of reinforcement have caused the bond fracture to begin deeper inside the footing which leads pullout at base to become greater. Based on the comparison between the behavior of C1-1 and C-5, reinforcement of tri-layer in C1-1 has one more layer than that in C1-5, it is clarified that the reduction influence from bar-to-bar become greater in C1-1 leading to its relative deeper depth of bond fracture.

6. CONCLUSIONS

Based on the experiment and analysis on C1-1 and C1-5, following conclusions have been drawn:

(1) As for C1-1 specimen, pullout displacement measured by displacement meter reaches 1.35 mm and 3.79 mm in average, and by strain gauge reaches 1.04 mm and 3.25 mm in average at 1δy and 2δy respectively. It can be obtained that the measured pullout increases by about 3 times when the column top displacement increases by twice. However, the contributed ratio by pullout keeps steady and reaches 28% in average. On one hand it may be caused by increased distance of neutral. On the other hand, cracks on the pier body becomes more and larger after the column displacement exceeds yield displacement.

(2) As for C1-5 specimen, pullout displacement measured by displacement meter reaches 1.59 mm and 4.85 mm in average, and by strain gauge reaches 1.24 mm and 3.12 mm in average at 1δy and 2δy respectively. It can be also obtained that the measured pullout increases by about 3 times when the column top displacement increases by twice. However, the contributed ratio by pullout keeps steady and reaches 30% in average. C1-5 reaches relative greater pullout and it also has larger distance neutral axle due to its relative greater scale, which causes the base rotation in both C1-1 and C1-5 is similar with each other. As the yield displacement is almost same in both C1-1 and C1-5, in the column top displacement, contributed ratio of base rotation caused by pullout reached about 30% steadily.

(3) Analysis considering the bar-to-bar reduction with close lapped spacing and layer spacing has well reappeared the experiment of both C1-1 and C1-5. Analysis considering bar-to-bar reduction shows that the bond fracture happed deeper, which is solved as -1.427 m and -1.444 m averagely for C1-1 and C1-5, than that in analysis just considering single bar. Multi-layer of reinforcement have caused the bond fracture to begin deeper inside the footing which leads pullout at base to become greater. Moreover, the reduction influence from bar-to-bar become greater in C1-1 which has one more layer that C1-5 leading to its relative deeper depth of bond fracture.

References

(1) Ukon, H., et al.: Large-scale Shake Table Experiment on a Component Model (C1-1 model) Using E-Defense, Technical Note of The National Research Institute for Earthquake Science and Disaster Prevention, No.331, 2009

(2) Ukon, H., et al.: Large-scale Shake Table Experiment on a Component Model (C1-5 model) Using E-Defense, Technical Note of The National Research Institute for Earthquake Science and Disaster Prevention, No.369, 2012

(3) Chou, L., et al.: Bond Characteristics in Post-yield Range of Deformed Bars, J. of JSCE, No.378/V-6, pp.213-220, 1987.2

(4) Ishibashi, C., et al.: Study on Deformation Capacity of Reinforced Concrete Bridge Piers under Earthquake, J. of JSCE, No.390/V-8, pp.57-65, 1988.2